GMR
The Original

DEVELOPMENT, OPTIMIZATION AND PHARMACOLOGICAL EVALUATION OF OLIVE OIL-BASED CURCUMIN NANOEMULSION WITH ARQ-E-MAKO AND ARQ-E-KASNI AGAINST DIETHYLNITROSAMINE-INDUCED HEPATOCELLULAR CARCINOMA IN RATS

Mohd Yusuf[1,2], Badruddeen[1*], Zeashan Hussain[2], Juber Akhtar[1], Mohammad Irfan Khan[1], Mohammad Ahmad[1]

[1]Faculty of Pharmacy, Integral University, Lucknow-226026, Uttar Pradesh, India.
[2]Mahatma Gandhi Institute of Pharmacy, Junabganj, Kanpur Road, Lucknow-226401, Uttar Pradesh, India
[*]**Corresponding author:** Dr. Badruddeen, E-mail: badarmiracle@gmail.com

ABSTRACT

OBJECTIVE: Development and optimization of the olive oil-based curcumin nanoemulsion and its evaluation with Ark-e-mako and Ark-e-kasni against diethylnitrosamine induced hepatocellular carcinoma in rats.

MATERIAL AND METHODS: The nanoemulsion was constructed via an aqueous titration method. Distilled water served as the aqueous phase, and olive oil, tween 80, and ethanol served as the oil phase, surfactant, and co-surfactant. Nanoemulsion was characterized on the basis of particle size and stability study. Further, in vivo pharmacological study, the rats were divided into 7 groups (each 6). The hepatocellular carcinoma (HCC) was induced in all groups except in group I. The HCC was induced by administering diethynitrosamine (DEN) (200 mg/kg, i.p.) single dose and carbon tetrachloride (CCl4 3 ml/kg, i.p.) weekly for 6 weeks. At the end of the six-week, blood was collected from each group through retro orbital puncture and subjected to the alpha fetoprotein (AFP) and carcinoembryonic antigen (CEA) test. After confirmation of HCC in rats, all the treated groups I, II, III, IV, V, VI and VII were administered orally with Vehicle (Normal saline), Methotrexate, Curcumin nanoemulsion, Arq-e-mako, Arq-e-kasni and combination of curcumin nanoemulsion, Arq-e-mako, Arq-e-kasni respectively, onec a day for 8 weeks. After the completion of experimental period the rats were anesthetized (Ketamine 60 mg/kg, i.p.) and blood sample was collected through cardiac puncture for estimation of HCC markers such Alpha feto protein and Carcinoembryonic antigen and other biochemical parameters (SGOT, SGPT, ALP, Total Protein etc). Further rats were euthanized; liver were carefully removed and put in a 10% neutral buffered formalin solution for biochemical and histological examination.

RESULTS: The refined formulation exhibited an average particle size of 200 nm and a zeta potential of -13.76. The stability of the formulation under stressful condition was found to be stable. The impact on percentage body weight variation across several treatment groups revealed a notable rise in body weight relative to the disease control. The treated groups had a notable reduction in biochemical parameters of SGPT, SGOT, and ALP when contrasted with the disease control group. The treated groups also exhibit a notable reduction in alpha feto protein and carcinoembryonic antigen levels compared to the disease control groups. Histopathological observations indicate enhancement in cellular architecture within the treatment group relative to the disease control groups.

CONCLUSION: The overall results indicate that the optimised formulation when administered along with Arq-e-Mako and Arq-e-Kasni has promising hepatoprotective and anticancer potential by improving body weight, liver function biomarkers, tumour related indicators and histological changes.

KEYWORDS: Nanoemulsion, Hepatocellular carcinoma, Ketamine, Diethyl nitrosamine, Alpha Fetoprotein and Carcinoembryonic antigen

INTRODUCTION

The predominant kind of primary liver cancer, hepatocellular carcinoma (HCC), is a leading global cause of cancer mortality. As to Balogh et al. (2016), this is the tenth commonest reason for cancer mortality in the Unites state. A significant number of patients still encounter late-stage diagnoses, even with enhancements in cancer surveillance and diagnosis [Zaafar et al., 2024]. Surgical removal, liver grafting, liver-targeted interventions, and systemic therapies represent several treatment modalities for HCC [Balogh et al., 2016].

The prevalent modalities for cancer treatment nowadays include of radiation, chemotherapy, and surgical procedures. The general non-selectivity or non-specificity of the predominant anticancer treatments now in use for tumour cells and tissues is a key concern that restricts their efficiency. Scholars have sought to utilise natural herbal medicines, phytomedicines, and therapeutically beneficial phytochemicals from natural origins for cancer therapy, motivated by several shortcomings of current anticancer treatments and the quest for alternative effective regimens. Plant-based herbal solutions and phytochemical elements sourced from vegetation have been utilized for an extended period to address many human health issues. Curcumin (CUR), among several polyphenols known for their anticancer capabilities, has shown outstanding anticancer effectiveness against multiple cancer types.

The rhizomes of Curcuma longa are the origin of curcumin, a hydrophobic polyphenolic substance [Srimal & Dhawan, 1973].
Although curcumin is beneficial, it has certain disadvantages that restrict its utilization in cancer treatment, including low bioavailability and poor solubility [Rageh et al., 2023]. Thus, it is imperative to discover a delivery method that can augment drug solubility and bioavailability, address resistance, and especially aim at cancer tissues. In conclusion, this could refine the treatment of HCC by elevating its pharmacological potency and reducing negative effects. The potency of anticancer interventions has markedly enhanced owing to nanotechnology, a pioneering discipline that has been applied for several decades [Barenholz, 2012]. Arq-e-mako and Arq-e-kasni have shown hepatoprotective effects [Parween & Begum, 2017].

MATERIAL AND METHODS:
Curcumin, Olive oil, Tween 80, Ethanol were purchased from Yarrow Chem Product, Mumbai, Diethylnitrosamine (DEN) was purchased from Sigma Aldrich. All remaining compounds were of analytical quality and utilised as needed.

Animals
The adult male Wistar rats weighing 150-180 gm, were purchased from CDRI, Lucknow and kept in the Animal House Facility at Mahatma Gandhi Institute of Pharmacy (MGIP) under standard environmental conditions with unlimited access to standard food and water.
Animals were maintained under properly controlled housing conditions and fed with a normal commercial pellet diet obtained from M/s Hindustan Foods Ltd. (Bangalore, India). This experiment received ethical approval from the Institutional Animal Ethics Committee (IAEC) of the MGIP, Lucknow (Approval No: MGIP/IAEC/04/23).

Nanoformulation development and its characterization
The ability of curcumin to dissolve in various oils is a significant determinant in the selection of oils for nanoemulsion creation. This initial formulation research employed multiple oils, including castor, coconut, olive, almond, and sesame oils. A vortex mixer facilitated the integration of an excess of medication in 2 millilitres of each respective oil independently contained in 5 milliliters rubber plugged vials [U. Ahmad et al., 2017]. The vials were stirred in an isothermal shaker (IKA® KS 400i, Staufen, Germany) at 25 ± 1.0 °C for 72 h to reach equilibrium. Following extraction from the shaker, the equilibrated nanoemulsions were subjected to centrifugation for 15 minutes at a speed of 10,000 rpm with a centrifuge (REMI, Mumbai, India). The supernatant was clarified by filtration using a 0.45 µm membrane filter. The quantities of curcumin in different oils were assessed with a spectrophotometer adjusted to 288 nm.

Pseudo ternary phase diagram study
Smix facilitated the integration of cosurfactant (Ethanol) and surfactant (Tween 80) across a range of volumetric ratios (1:0, 1:1, 1:2, 1:3, 2:1, 3:1, 4:1, etc.). For an in-depth study of the phase diagrams pertaining to nanoemulsion formation, these Smix ratios were designated to depict higher cosurfactant concentrations compared to surfactant and greater surfactant concentrations compared to cosurfactant [Kommuru et al., 2001]. According to the solubility analysis, olive oil was used as the oil phase. Olive oil and a designated Smix ratio were carefully agitated in assorted glass vials at volume ratios from 1:9 to 9:1 for every phase diagram. The research involved the formulation of sixteen unique oil and Smix ratios (1:9, 1:8, 1:7, 1:6, 1:5, 1:4, 1:3.5, 1:3, 1:2.33, 1:2, 1:1.5, 1:1, 1:0.66,1:0.43,1:0.25, and 1:0.11). The pseudo-ternary phase boundaries were determined by the aqueous phase titration method. Each oil-Smix combination was titrated separately with the aqueous phase [Lawrence et al., 2000]. A concentration of water varying from 5% to 95% of the total volume was realised by modifying the volume of aqueous phase injected at intervals of around 5%. The ratio of each nanoemulsion element at each 5% addition was assessed for the inclusion of the aqueous phase. For instance, an oil-Smix ratio of 1:9, the aqueous phase was added dropwise using micropipette in roughly 5% volume increments with concomitant vortex mixing. The formulation visual appeal is demonstrated by the easy scaling of proportions made possible by its thermodynamic stability.
1. Oil/water nanoemulsions that are transparent and readily flowable
2. Nanoemulsion gel, or translucent gel
3. Cloudy or milky: emulsion
4. Emulgel, a milky gel

The remaining oil–Smix combinations were tested similarly. A pseudo-ternary phase diagram was produced with oil, water and fixed-ratio surfactant-cosurfactant blend as the axis (Figure 2) showing the phase boundaries. A distinct phase diagram was created for each Smix ratio, and was utilised to document the visual observations corresponding to each phase diagram.

Thermodynamic stability tests
A series of thermodynamic stability evaluations were executed on a group of formulations using centrifugation, temperature variations, and freeze-thaw cycles.
Heating–cooling cycle: For at least 48 hours throughout each temperature cycle, the produced formulations were maintained at 45 ^{0}C and 0 ^{0}C.

Centrifugation tests: The physical stability was evaluated by centrifuging the formulations at 5,000 rpm for 30 min (REMI, Mumbai, India) and observing any phase separation, creaming or cracking.
Freeze-thaw cycle: For a maximum of 24 hours, the produced preparations were subjected to two distinct temperatures, namely -20 °C and 200 °C. Each batch of formulation underwent three of these cycles in order to improve the estimation of accelerated stability studies. Formulations with the highest stability were chosen for additional research [Akhtar et al., 2015].

Preparation of curcumin-loaded nano emulsions (CLN) by aqueous titration method
The curcumin-loaded nanoemulsion was formulated using 20 mg of curcumin, which is solubilized in oil (10%, 15%, 20%, and 25% v/v). Further, the oil was combined with the appropriate Smix ratio using a vortex mixer, and then the aqueous phase was added to achieve nanoemulsion.

Curcumin Nano Emulsion: Physicochemical Analysis and Assessment
Visual Examination
The distinction between CLN and macroemulsion was made by visual observation.

Measurement of dynamic light scattering (DLS)
The mean droplet size and polydispersity index (PDI) of CLN were determined by using the DLS technique, which involves the use of a zetasizer ZS 90 (Malvern Instruments, Worcestershire, UK) to monitor the changes in the light scattering due to the Brownian motion of the particles. Light scattering was observed at 25 °C and at an angle of 90°. The aliquot was immediately placed into the module after being diluted with distilled water and subjected to filtration using a 0.45 µm membrane filter [Akhtar et al., 2015].

Electron microscopy via transmission (TEM)
Using a JEOL JEM1400 Transmission Electron Microscope, the surface morphology of CLN was examined [Akhtar et al., 2015]. The nanoemulsion was diluted in distilled water (1:100, v/v) and filtered through a 0.22 µm membrane. Then a drop of the sample was deposited on a copper grid coated with carbon, negatively stained with 2% phosphotungstic acid for 30 sec. dried and a cover slip was placed on the dried coated grid on a slide. A 200 kV light microscope was used to examine the slide [Ahmad et al., 2019].

Stability studies
The optimized curcumin nanoemulsion formulations underwent accelerated stability studies for these formulations were stored in stability chambers (Thermolab, Mumbai, India) under three conditions, 25 ± 2 °C/60 ± 5% RH, 40 ± 2 °C/65 ± 5% RH and 60 ± 2 °C/75 ± 5% RH. The samples were stored in sealed glass bottles and analysed at pre-determined time intervals (0, 30, 60 and 90 days) for droplet size, polydispersity index (PDI) [Akhtar et al., 2014].

In Vivo Pharmacological Study:
Experimental Design
All rats were randomly divided into 7 groups (each 6). The HCC was induced in group II, III, IV, V, VI, VII with a single dose of diethylnitrosamine (DEN) (200 mg/kg, i.p.). One week after the administration of DEN, (CCl_4 3 ml/kg, i.p.) was administered weekly for six weeks as a promoter for carcinogenesis. At the end of the six-weeks, blood was collected from each group through retro orbital puncture and subjected to the Alpha fetoprotein (AFP) and Carcinoembryonic antigen (CEA) test. After confirmation of HCC, all the groups were treated as per given treatment schedule (Table 1) for 8 weeks.

Table 1: Treatment schedule:

Groups (N=6)	Treatment	Dosage, Route of administration, & duration
I (NC)	Vehicle (0.9% normal saline)	5 ml/kg, p.o. once a day for 8 weeks
II (DC)	HCC rats + Vehicle	5 ml/kg, p.o. once a day for 8 weeks
III (STD)	HCC rats + MTX	5 mg/kg, p.o. once a day for 8 weeks
IV	HCC rats + Curcumin nanoemulsion	5 ml/kg, p.o. once a day for 8 weeks
V	HCC rats + Arq-e-Kasni	5 ml/kg, p.o. once a day for 8 weeks
VI	HCC rats + Arq-e- Mako	5 ml/kg, p.o. once a day for 8 weeks
VII	HCC rats + Curcumin nanoemulsion + Arq-e-Kasni + Arq-e-Mako	2.5 ml/kg + 2.5 ml/kg + 2.5 ml/kg, p.o, once a day for 8 weeks

N= number of animals, NC: Normal Control, DC: Disease Control, STD: Standard, HCC: Hepatocellular Carcinoma, MTX: Methotrexate

Each 5 ml nanoemulsion contain 400 mg curcumin.
After the completion of experimental period the rats were anesthetized (Ketamine) (60 mg/kg, i.p.) and blood

sample was collected through cardiac puncture for estimation of HCC markers such as alpha feto protein and carcinoembryonic antigen and other biochemical parameters (SGOT, SGPT, ALP, Total Protein etc). Further animals were euthanized; liver were carefully removed and put in a 10% neutral buffered formalin solution for biochemical and histological examination.

Evaluation of biochemical parameters

The collected blood samples were centrifuged using a refrigerated centrifuge machine, and serum was collected and used for the estimation of different biochemicals. Serum was employed to measure hepatic enzymes (aspartate aminotransferase (AST) and alanine aminotransferase (ALT)) and tumour markers (carcinoembryonic antigen (CEA) and alpha-fetoprotein (AFP)) [Talerman et al., 1976]. The Lowry et al. approach was utilised to assess the total protein levels in the liver. The liver tissue homogenate served to evaluate the activity of the antioxidant enzymes reduced glutathione (GSH), catalase (CAT), and superoxide dismutase (SOD) [Goc et al., 2017].

Histopathological evaluation

Liver tissue samples (6 mm in size) were fixed in 10% phosphate-buffered formalin and embedded in paraffin wax. Sections were then cut to a thickness of 5 µm, stained with Hematoxylin and Eosin, and analyzed under a photographic high-resolution microscope.

Statistical analysis

For each set of six animals, the data were presented as mean ± SEM. One-way ANVOA was used for statistical analysis, and Dunnett's test was used to compare each group to the control (Graph Pad Instat, USA).

RESULTS:

Solubility studies

Solubility study was performed to identify an ideal oil phase which can provide maximum curcumin loading. High solubility of the drug in the lipid phase is important to avoid precipitation and to keep curcumin in a completely solubilized form in the nanoemulsion. The oil phase test revealed that olive oil had the greatest curcumin solubility at 101.2 mg/ml, followed by castor oil at 64 mg/ml, coconut oil at 25.32 mg/ml, almond oil at 23 mg/ml, and sesame oil at 15 mg/ml (Figure 1). Olive oil was selected as an optimum oil phase for the development of formulation.

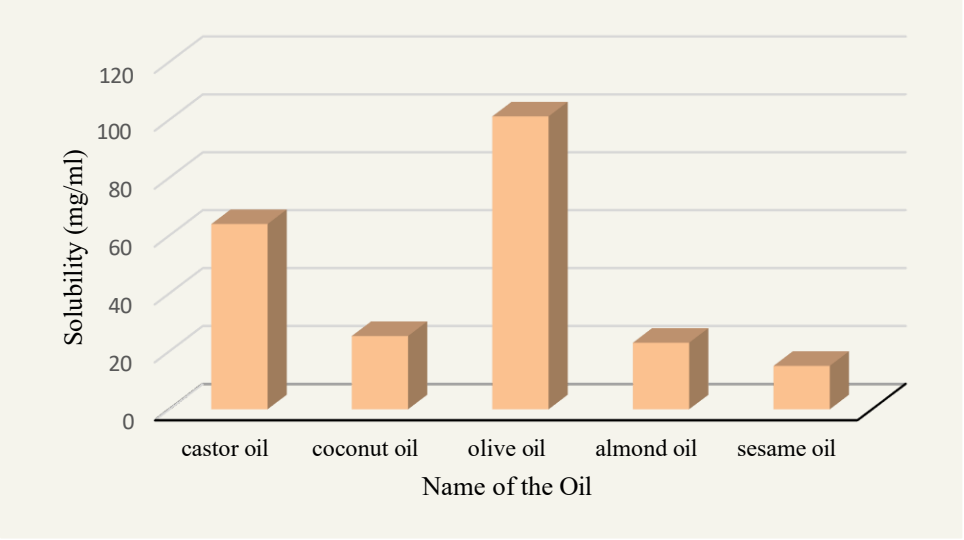
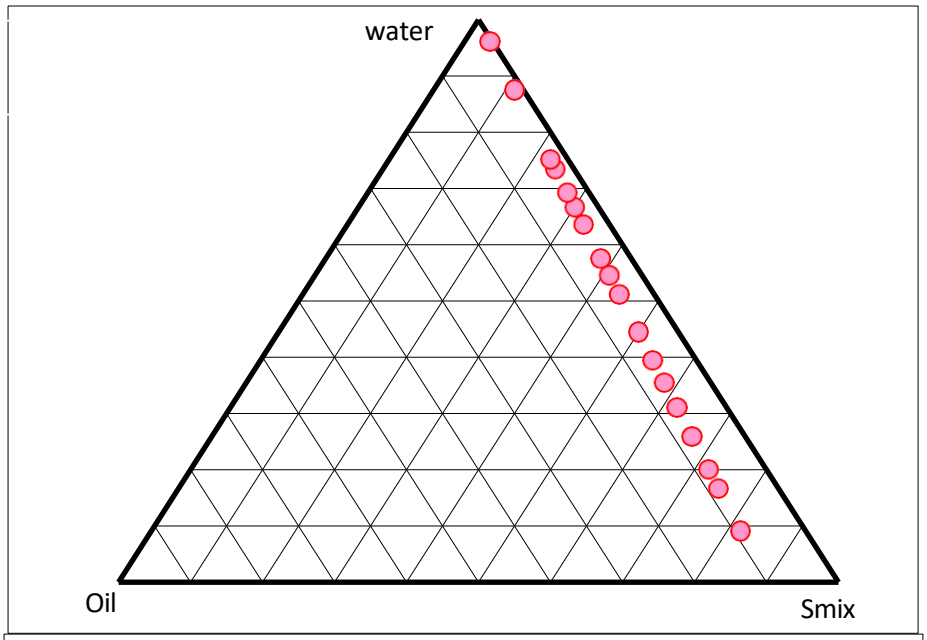


Figure. 1 Curcumin exhibiting highest solubility in olive oil

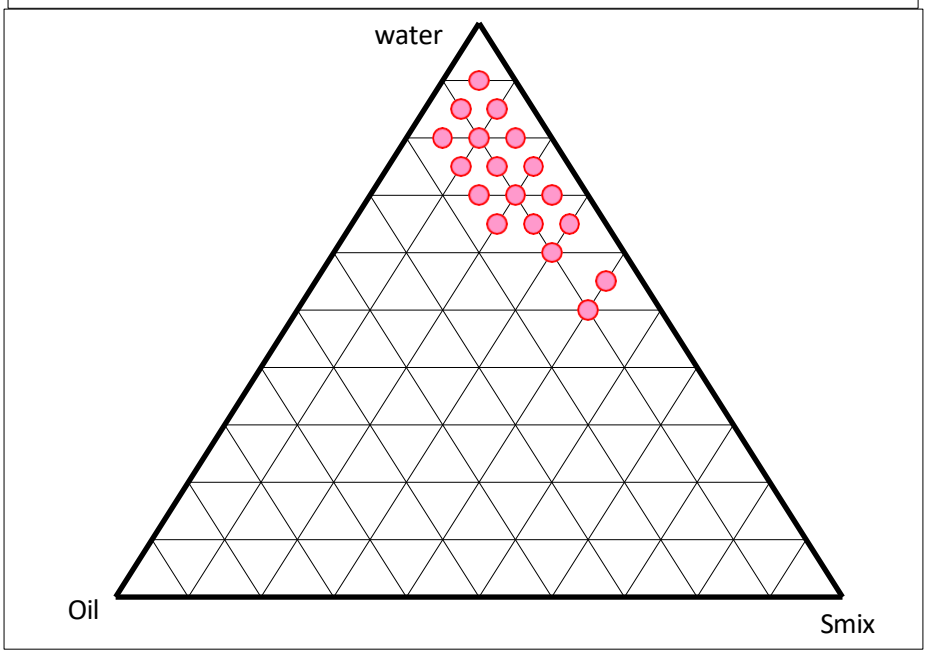
Pseudo ternary phase diagram study

The nanoemulsion region of the system Olive oil–Tween 80/Ethanol–Water was determined by mapping a pseudo-ternary phase diagram using the aqueous titration method. Each dot represents a formulation with different ratios of oil, Smix and water. Phase diagram of transparent and stable nanoemulsion formulations was plotted. It was observed that a narrow band of nanoemulsion region extends from the water-rich region towards higher Smix concentrations indicating a high dependence of nanoemulsion formation on the surfactant/co-surfactant concentration. Stable nanoemulsions with relatively low oil concentrations and moderate to high Smix levels were obtained, indicating that tween 80 and ethanol reduced the oil-water interfacial tension and promoted the spontaneous formation of nano-sized droplets. Conversely, formulations with higher oil concentrations or lower Smix concentrations were not able to form stable nanoemulsions and were not considered in the nanoemulsion region due to turbidity or phase separation. The results indicate that the nanoemulsion region is widened and the solubilising capacity of the oil phase is increased with the increase of Smix concentration (Figure 2).

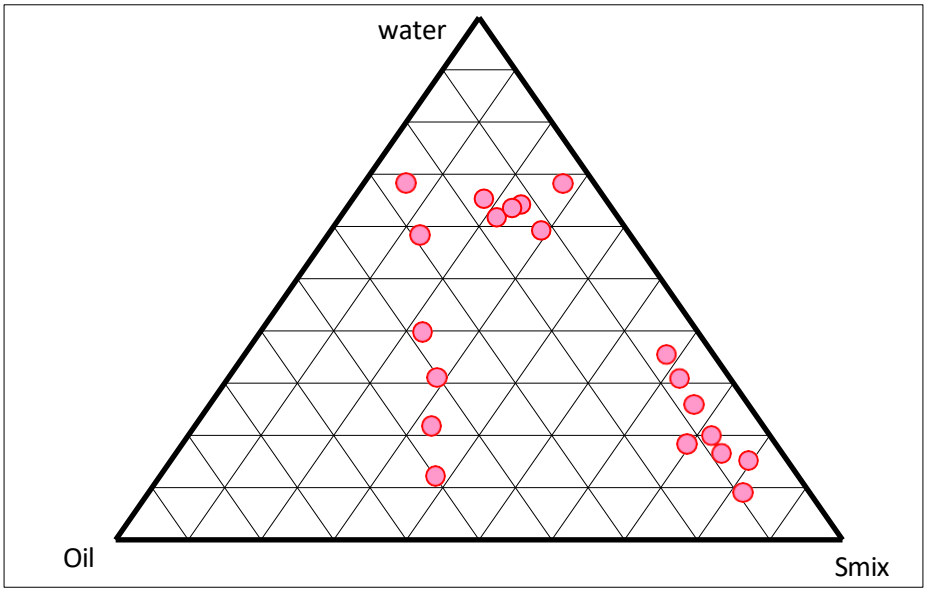
F1



F2



F3



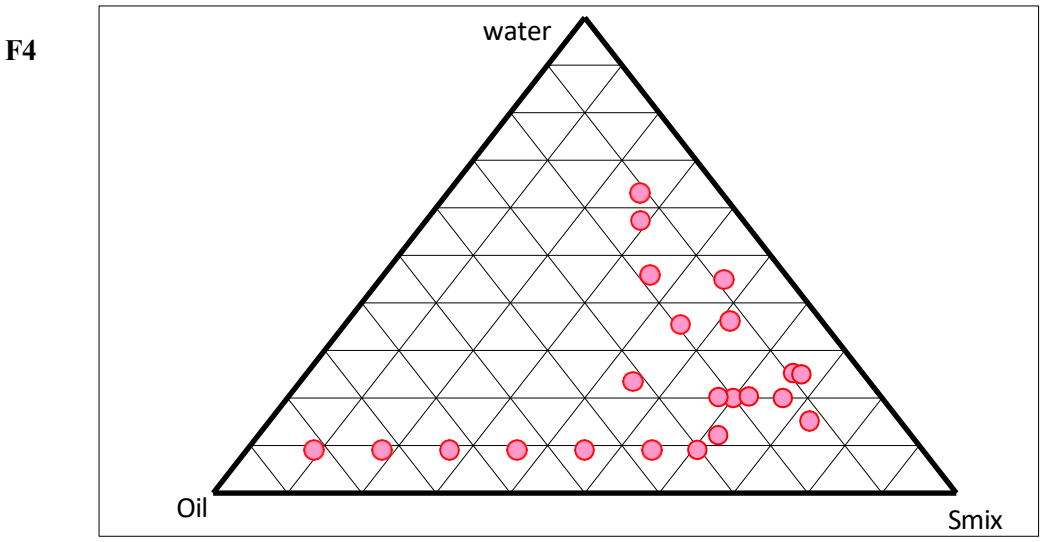


Figure 2. Pseudoternary phase diagrams of curcumin nanoemulsions F1 (Smix 1:0), F2 (Smix 1:1), F3 (Smix 2:1), and F4 (Smix 1:2).

Thermodynamic stability Test:
Thermodynamic stability experiments were performed on the produced formulations following nanoemulsion optimization. Under stressful conditions, nanoemulsions continue to be stable. The stability of the formulations was assessed using three tests: freeze-thaw cycles, centrifugation, and heating/cooling cycles. The test observations are listed in (Table 2).

Table 2. Thermodynamic stability tests of prepared nanoformulation.

Formulation	Smix ratio	%Oil	%Smix	%Water	Thermodynamic stability tests			Inference
					Heating/cooling	Centrifugation	Freeze-Thaw	
NE1	**2:1**	9.09	81.81	9.09	✓	✓	✓	**Passed**
NE2		8.33	75	16.66	✓	✓	✓	**Passed**
NE3		8	72	20	**X**	_	_	**Failed**
NE4		7.40	66.66	25.92	✓	✓	✓	**Passed**
NE5		6.89	62.06	31.03	✓	✓	✓	**Passed**
NE6		6.45	58.06	35.48	**X**	_	_	**Failed**
NE7		6.06	54.54	39.39	✓	✓	✓	**Passed**
NE8		5.55	50	44.44	**X**	_	_	**Failed**

Preparation of Curcumin Nanoemulsion
The refined formulations that successfully met all criteria and contained minimal surfactant concentrations were utilised for the integration of curcumin.
Characterization and evaluation of nanoemulsion
The selected Curcumin nanoemulsion was analysed and assessed based on the subsequent criteria.
Visual appearance
The prepared curcumin nanoemulsion was clear and optically transparent and did not show any turbidity as opposed to the conventional macroemulsions which have a characteristic milky appearance.
Dynamic light scattering (DLS) measurement
Dynamic Light Scattering (DLS) was used to determine the polydispersity index (PDI), zeta potential and droplet size distribution of nanoemulsions [Parveen et al., 2011]. NE4 formulation had a mean droplet size of 200 nm. The optimization of the ratio of oil, S_{mix} and aqueous phase produced stable nanoscale droplets, highlighting the importance of fine-tuning the proportions of surfactant, co-surfactant and oil to attain minimum droplet diameter

and colloidal stability (Figure 3).

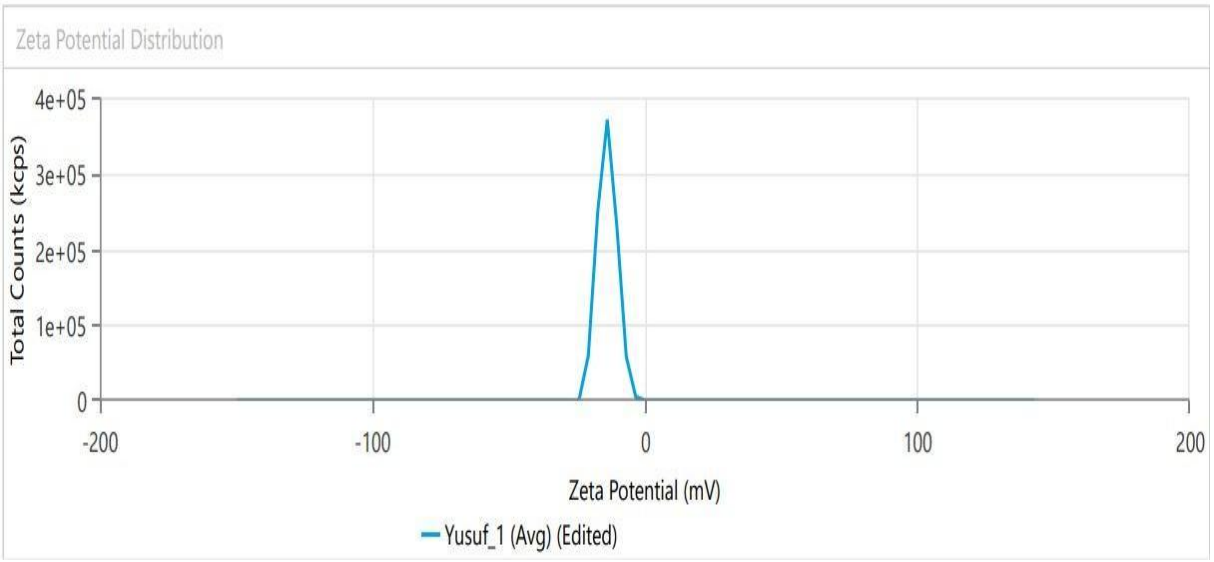


Figure 3: Zeta Potential of Curcumin Loaded nanoemulsion

TEM

Image of NE4 showed that curcumin loaded nanoemulsion droplets were 200nm (Figure 4).

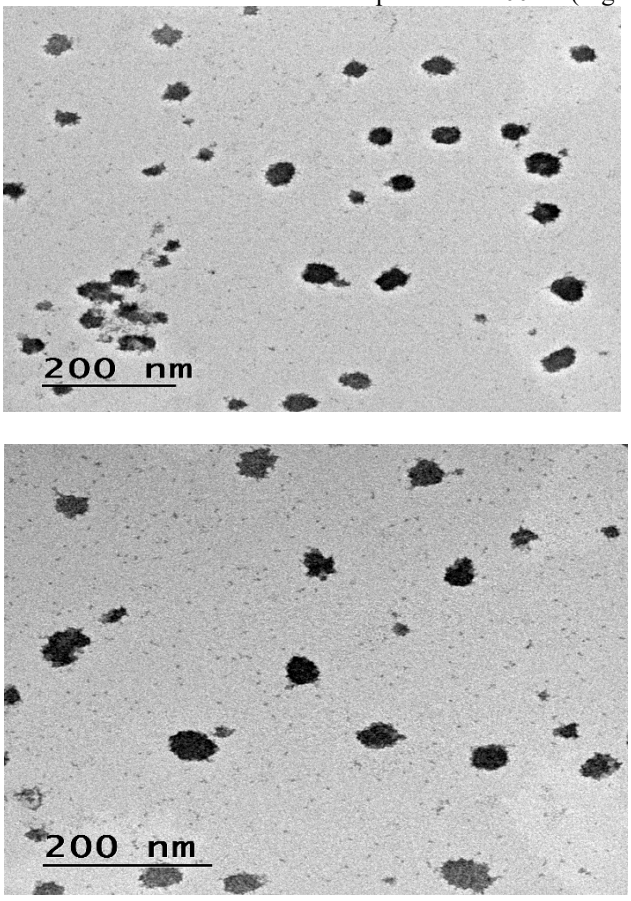


Figure 4: Electron microscopy of Curcumin loaded nanoemulsion

Accelerated stability studies

Nanoemulsion stability was demonstrated by the absence of phase separation and flocculation. In contrast to optimized curcumin nanoemulsion formulations at day zero, data collected at temperatures of 60 ^{0}C/65 RH for 90 days revealed increased droplet size but decreased transparency.

In Vivo Pharmacological Study Results:

Effect on body weight variation (%) and relative liver weight.

Table 3 represents the effect of different treatments on the body weight of controlled and experimental groups of rats. Final changes in the body weight of rats in each group were examined on last day of the experimental periods

to evaluate the effects of different treatment. Group II rats showed significant ($p<0.001$) loss in body weight as compared to group I (Normal control) rats. Treatment group III showed significant ($p<0.001$) gain in body weight as compared to Group II rats. Treatment of DEN induced HCC rats in groups IV, V, VI showed significant ($p<0.05$) gain in body weight as compared to Group II rats while treatment of DEN induced HCC rats in group in VII group showed significant ($p<0.001$) gain in body weight as compared to Group II rats.

Table 4 represents the effect of different treatments on liver weights and relative liver weights of control and experimental groups of rats. Group II showed a significant ($P < 0.001$) increase in relative liver weight when compared to group I (Normal Control). Group III, IV, V VI and VII significantly reduced ($P < 0.01$) the relative liver weight as compared to group II. Group VII showed no significant change in body weight and relative liver weight when compared to the control group.

Table 3: Effect of olive oil-based curcumin nanoemulsion with Ark-e-mako and Ark-e-kasni against diethylnitrosamine induced hepatocellular carcinoma on body weight in HCC rats.

Groups	Initial body wt.	Final body wt.	% body wt. variation	
			Decrease	Increase
I	174.14 ± 0.47	193.5 ± 0.76	-	11.09± 0.27
II	165 ± 0.36	115.91 ±1.37	29.74 ± 0.89$^{\#\#}$	-
III	186.66 ± 1.58	157 ±2.63	15.8 ± 1.95**	-
IV	174.83 ± 0.70	146.6 ± 1.22	16.13 ± 0.85**	-
V	187 ± 1.0	134.2 ± 1.98	28.25 ± 0.69**	-
VI	191.5 ± 0.84	140.2± 0.43	26.78 ± 0.42**	-
VII	171.66 ± 1.9	154.11±1.28	10.18 ± 0.74**	-

All values were expressed as mean ± SEM. Significant difference between various groups (ANOVA) and individual comparison was done by Dunnett's t-test. $^{\#\#}p<0.01$=Significant, when compared with normal control (NC), $^{**}p<0.01$=Significant, when compared with Disease control (HCC).

Table 4: Effect of olive oil-based curcumin nanoemulsion with Ark-e-mako and Ark-e-kasni against diethylnitrosamine induced hepatocellular carcinoma on liver weight and relative liver weight in HCC rats.

Groups	Final Body wt. (g)	Liver wt. (g)	Relative liver wt. (Liver weight/100 g body wt.)
I	193.5 ± 0.76	9.31 ± 0.05	4.81 ±0.03
II	115.91 ±1.37	17.51 ± 0.28	11.27 ±0.19$^{\#\#}$
III	157 ±2.63	14.55 ± 0.21	9.28 ±0.20**
IV	146.6 ± 1.22	13.39 ± 0.38	9.14 ±0.31**
V	134.2 ± 1.98	12.46 ± 0.39	9.28 ± 0.64**
VI	140.2± 0.43	11.87 ± 0.24	9.06 ±0.20**
VII	154.11±1.28	10.72 ± 0.30	6.96± 0.20**

Values are expressed as mean ± SEM of 6 rats in each group.
P values: ##P<0.01 compared with group I
P value: ** P<0.001 compared with group II

Biochemical Parameters:

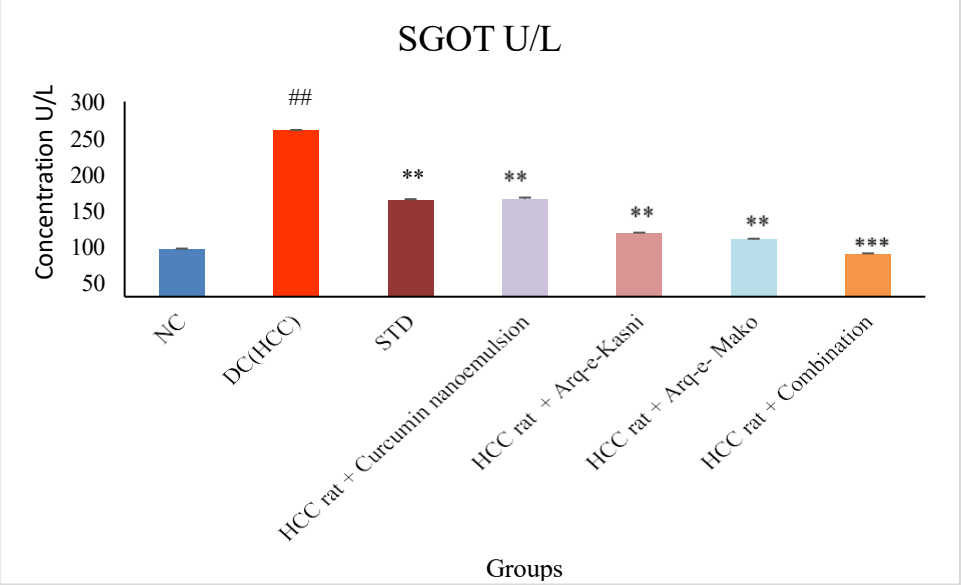
Effect on serum SGOT, SGPT and ALP

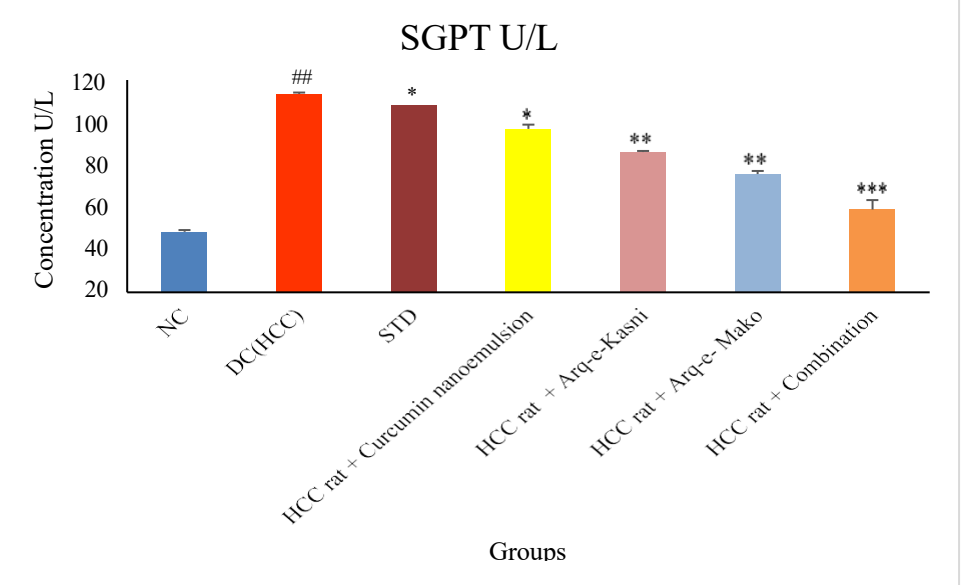
The effect of olive oil-based curcumin nanoemulsion, with Ark-e-mako and Ark-e-kasni, in diethylnitrosamine-induced hepatocellular carcinoma on liver injury markers in experimental rats is illustrated. The serum levels of AST (SGOT), ALT (SGPT), and ALP were markedly higher in Group II rats than in the control group I rats ($P<0.01$). Group III exhibited markedly ($P < 0.05$) decreased AST, ALT, and ALP levels relative to group II. Groups IV, V, VI, had markedly ($P < 0.01$) reduced AST, ALT, and ALP levels in contrast to group II. Group VII had markedly ($P < 0.001$) reduced AST, ALT, and ALP levels in contrast to group II.

Table 5: Effect of olive oil-based curcumin nanoemulsion with Ark-e-mako and Ark-e-kasni against diethylnitrosamine induced hepatocellular carcinoma on the liver injury markers in HCC rats.

Groups	AST/SGOT (U/L)	ALT/SGPT (U/L)	ALP (U/L)
I	73.77 ± 0.27	34.2 ± 1	60.16 ± 7.22
II	255.41 ± 0.85$^{\#\#}$	112.14 ± 0.79$^{\#\#}$	172.41 ± 2.8$^{\#\#}$
III	148.47 ± 1.46**	105.96 ± 1.86*	153.67 ± 2.92*
IV	150.07 ± 2.36**	92.39 ± 2.4*	145.28 ± 1.7**
V	98.13 ± 0.42**	79.29 ± 0.62**	75.92 ± 2.47***
VII	65.99 ± 0.67***	46.79 ± 5.34***	54.93 ± 7.49***
VI	88.25 ± 0.95**	66.85 ± 1.76**	56.63 ± 6.86***

Values are expressed as mean ± SEM of 6 rats in each group.
P values: ##P<0.01 compared with group I
P value: ** P<0.01 compared with group II
P value: * P<0.05 compared with group II
P value: *** P<0.001 compared with group II





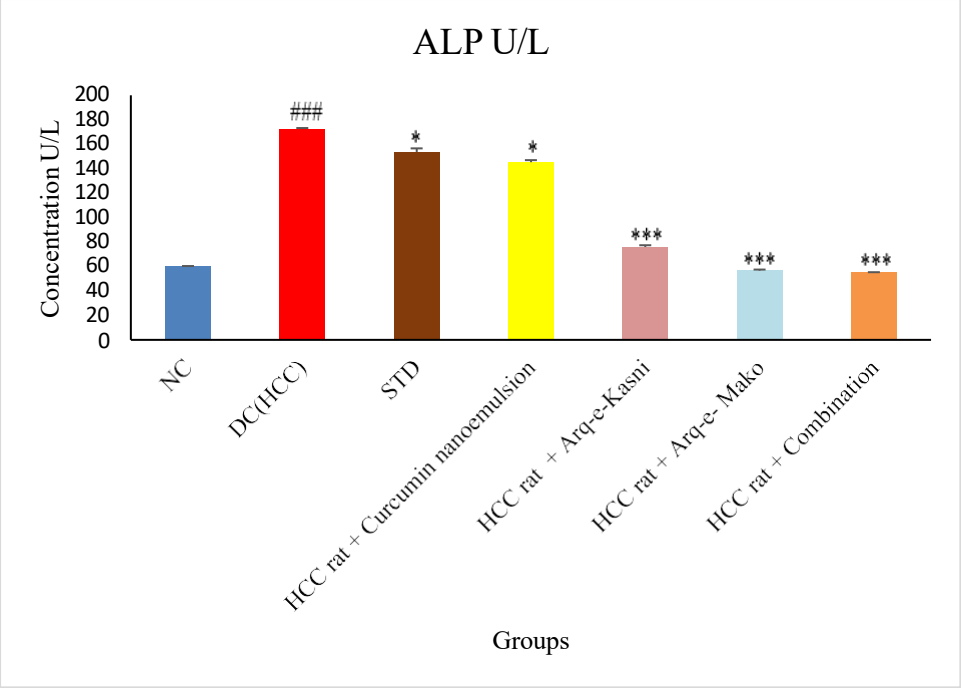


Figure 5: Effect of olive oil-based curcumin nanoemulsion with Ark-e-mako and Ark-e-kasni against diethylnitrosamine induced hepatocellular carcinoma on SGOT, SGPT and ALP liver markers in HCC rats.

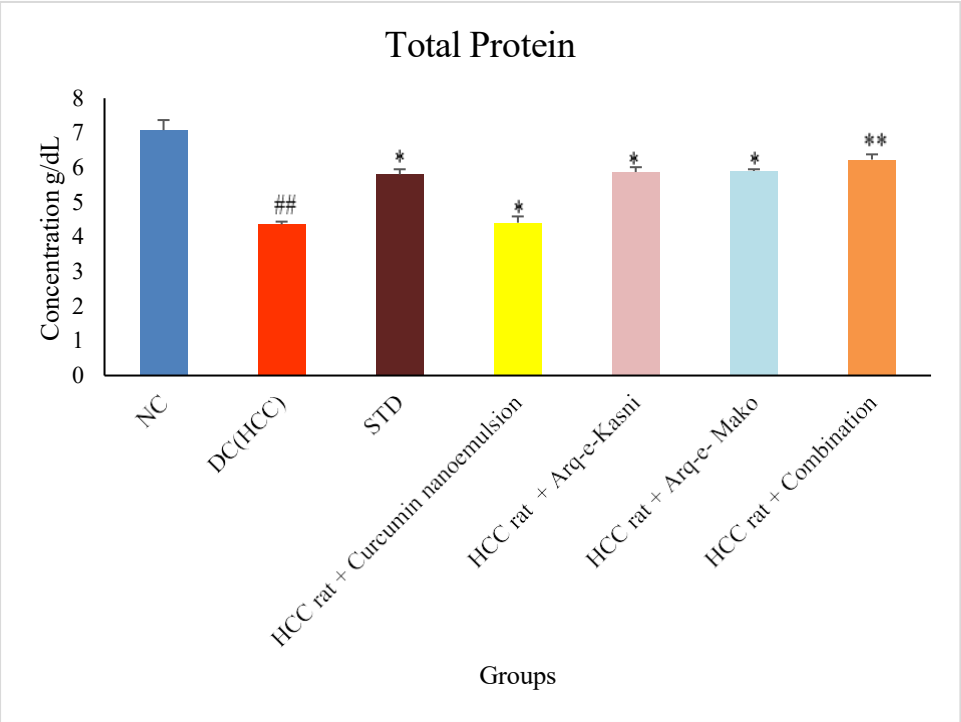
Effect on Total protein and Total Bilirubin:

Table 6: Represent the effect of olive oil-based curcumin nanoemulsion with Ark-e-mako and Ark-e-kasni against diethylnitrosamine induced hepatocellular carcinoma on the level of total protein and total bilirubin in HCC rats. It was found that total protein levels significantly ($P< 0.01$) decreased in group-II rats as compared to group-I rats while bilirubin levels significantly ($P< 0.01$) increased in group-II rats as compared to group-I rats. However, in group-III the levels of protein significantly ($P < 0.05$) increased while bilirubin level significantly ($P < 0.05$) decreased as compared to group-II. Groups IV, V and VI showed significantly ($P< 0.05$) increased the levels of total protein and decreased bilirubin as compared to group-II. Groups VII showed significantly ($P< 0.01$) increased the levels of total protein and decreased bilirubin as compared to group-II.

Table 6: Effect of olive oil-based curcumin nanoemulsion with Ark-e-mako and Ark-e-kasni against diethylnitrosamine induced hepatocellular carcinoma on Total Protein and Total Bilirubin.

Groups	Total Protein (g/dL)	Total Bilirubin (g/dL)
I	7.08 ± 0.29	0.44 ± 0.13
II	4.36 ± 0.08$^{\#\#}$	3.87 ± 0.36$^{\#\#\#}$
III	5.8 ± 0.15*	2.51 ± 0.31*
IV	4.41 ± 0.18*	2.25 ± 0.25**
V	5.87 ± 0.14*	1.15 ± 0.61**
VI	5.9 ± 0.05*	1.11 ± 0.21**
VII	6.23 ± 0.15**	0.54 ± 0.45***

Values are expressed as mean ± SEM of 6 rats in each group.
P values: ##P<0.01 compared with group I
P value: * P<0.05 compared with group II
P value: ** P<0.01 compared with group II
P value: *** P<0.001 compared with group II



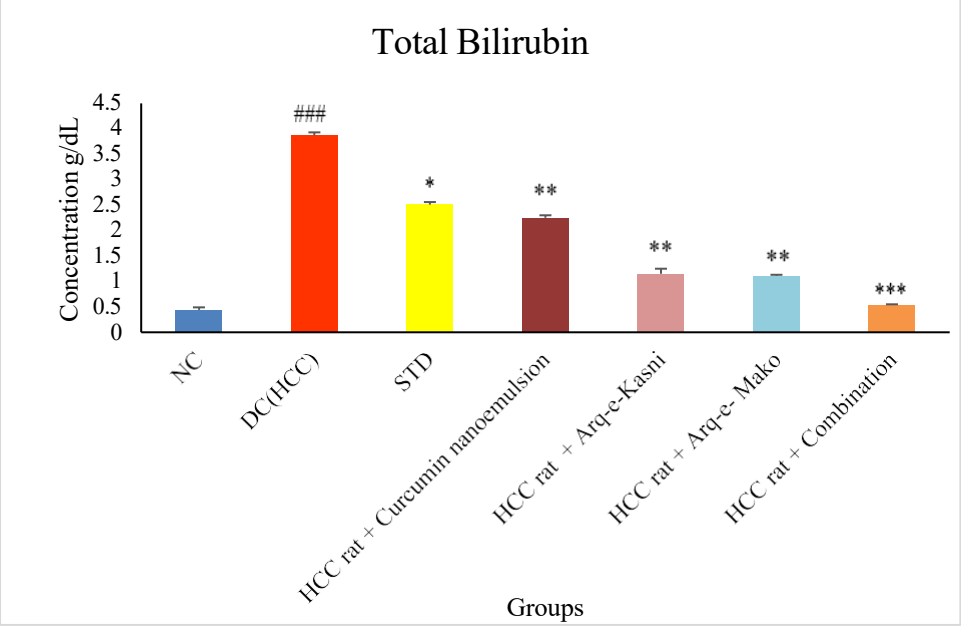


Figure 6: Represent the effect of olive oil-based curcumin nanoemulsion with Ark-e-mako and Ark-e-kasni against diethylnitrosamine induced hepatocellular carcinoma on total protein and total bilirubin level in HCC rats.

Effect on Liver cancer markers

The levels of the tumor markers α-feto protein (AFP) and carcinoembryonic antigen (CEA) are shown in **Table 7**. Group II rats showed significantly ($P < 0.01$) increased serum AFP and CEA compared to control group I rats. Treated group III showed significantly ($P < 0.05$) decreased AFP and CEA levels as compared to group II animals. Group IV, V, VI and VII showed significantly ($P < 0.01$) decreased AFP and CEA levels as compared to group II animals.

Table 7: Represent the effect of olive oil-based curcumin nanoemulsion with Ark-e-mako and Ark-e-kasni against diethylnitrosamine induced hepatocellular carcinoma on the level of total protein and total bilirubin in HCC rats.

Groups	Carcinoembryonic antigen (ng/ml)	Alfa- Fetoprotein (ng/ml)
I	1.39 ± 0.06	8.84 ± 0.01
II	7.04 ± 0.1$^{###}$	42.03 ± 0.27$^{###}$
III	3.82 ± 0.03***	14.8 ± 0.04***
IV	4.96 ± 0.12**	31.58 ± 0.19**
V	5.09 ± 0.17*	30.93 ± 0.61**
VI	4.49 ± 0.11**	26.27 ± 0.05**
VII	4.0 ± 0.12**	19.13 ± 0.02***

Values are expressed as mean ± SEM of 6 rats in each group.
P values: ###P<0.001 compared with group I
P value: ** P<0.01 compared with group II
P value: * P<0.05 compared with group II
P value: *** P<0.001) compared with group II

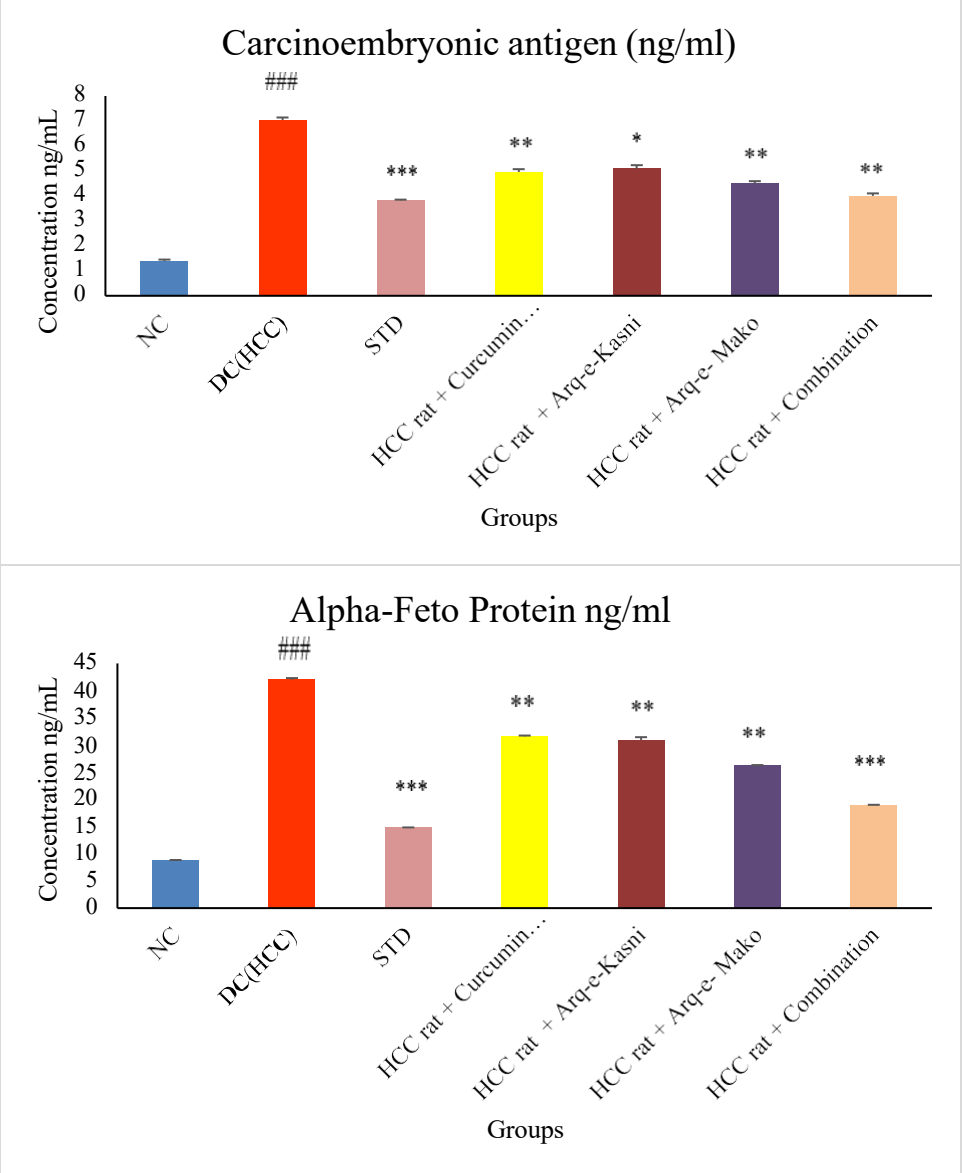


Figure 7: Represent the effect of olive oil-based curcumin nanoemulsion with Ark-e-mako and Ark-e-kasni against diethylnitrosamine induced hepatocellular carcinoma on the α-fetoprotein (AFP) and carcinoembryonic antigen (CEA) levels in HCC rats.

Effect on Antioxidant parameters:

Table 8 showed the levels of the reduced glutathione (GSH) and superoxide dismutase (SOD). Group II showed significantly (P< 0.01) decreased the levels of hepatic GSH and SOD as compared to control group I as compared to control group I. However, group III showed significantly (P < 0.001) increased levels of GSH, SOD when compared with group II. Group IV, V, VI and VII showed significantly (P < 0.001) increase levels of GSH and SOD when compared to group II rats.

Table 8: Represent the effect of olive oil-based curcumin nanoemulsion with Ark-e-mako and Ark-e-kasni against diethylnitrosamine induced hepatocellular carcinoma on the level of reduced glutathione and superoxide dismutase in HCC rats.

Groups	Reduced glutathione (nmol/mg of protein)	Superoxide dismutase (SOD units/mg of protein)
I	4.41 ± 0.1	141.08 ± 2.29
II	2.45 ± 0.03$^{\#\#}$	73.13 ± 0.4$^{\#\#}$
III	4.27 ± 0.26***	122.42 ± 0.71***
IV	4.34 ± 0.19***	136 ± 0.87***
V	5.3 ± 0.29***	146.06 ± 1.06***
VI	5.4 ± 0.54***	142.56 ± 1.26***
VII	6.1 ± 0.34***	156.06 ± 1.49***

Values are expressed as mean ± SEM of 6 rats in each group.
P values: $^{\#\#}$P<0.01 compared with group I
P value: *** P<0.001 compared with group II

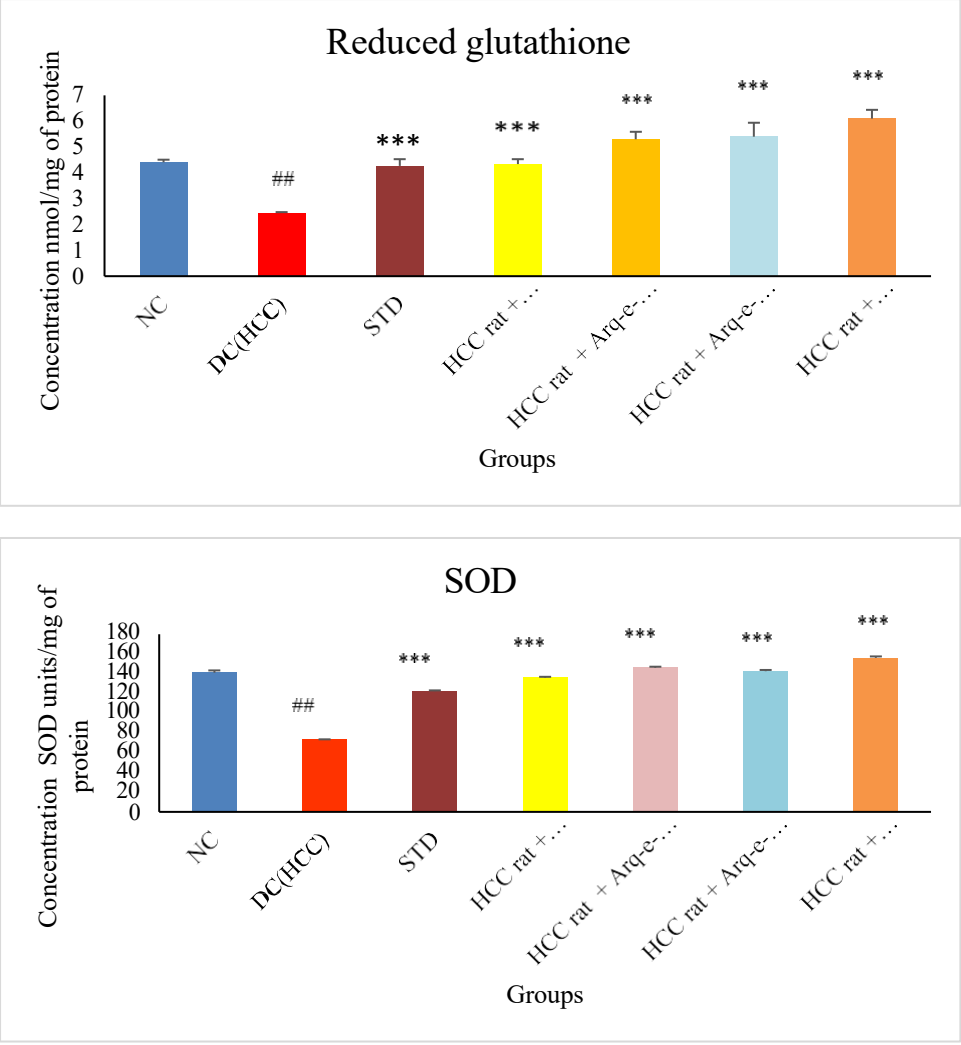


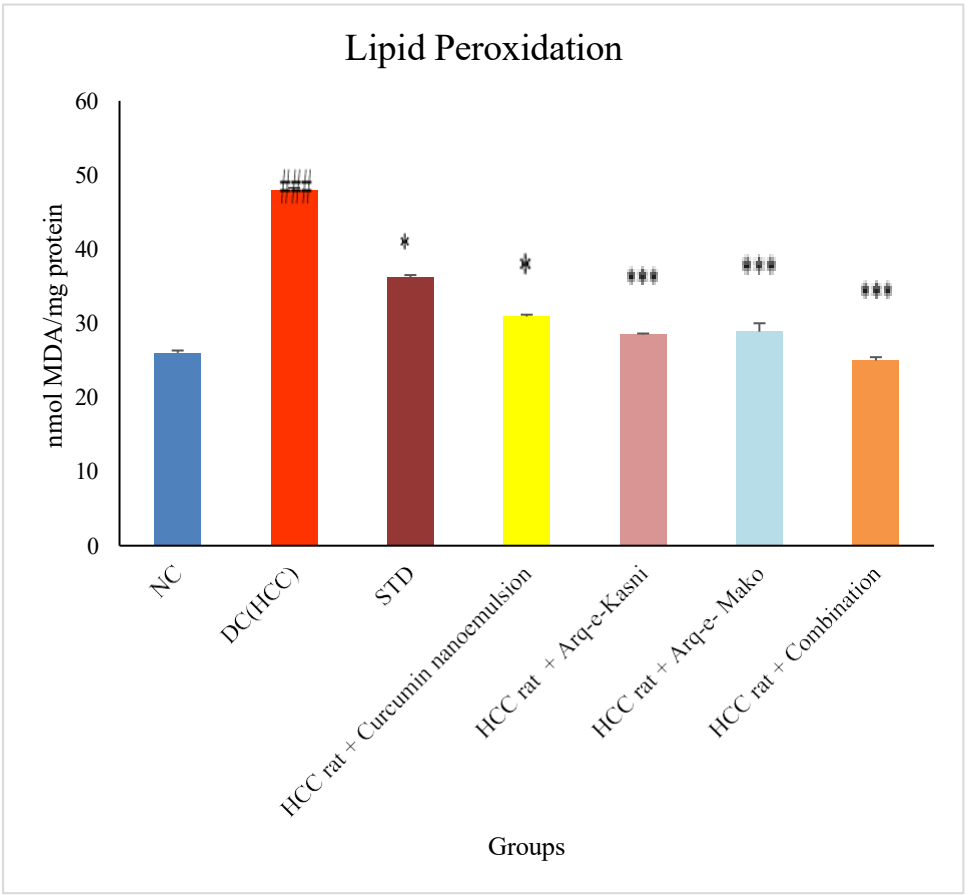
Figure 8: Represent the effect of olive oil-based curcumin nanoemulsion with Ark-e-mako and Ark-e-kasni against diethylnitrosamine induced hepatocellular carcinoma on the reduced glutathione and superoxide dismutase levels in HCC rats.

Table 9 showed the levels of the Lipid peroxidation (LPO) and Catalase (CAT). Group II showed significantly (P< 0.001) increased the levels of LPO as compared to normal control group I. However, group III showed significantly (P < 0.05) decreased levels of LPO when compared with group II. Group IV, V, VI and VII showed significantly (P < 0.001) decrease levels of LPO when compared to group II rats.
While Group II showed significantly (P< 0.001) decreased levels of CAT as compared to control group I. However, group III showed significantly (P < 0.05) increased levels of CAT when compared with group II. Group IV, V, VI and VII showed significantly (P < 0.001) increased levels of CAT when compared to group II rats.

Table 9: Represent the effect of olive oil-based curcumin nanoemulsion with Ark-e-mako and Ark-e-kasni against diethylnitrosamine induced hepatocellular carcinoma on the Lipid peroxidation and Catalase in HCC rats.

Groups	Lipid Peroxidation (nmol MDA/mg protein)	Catalase Activity (U/mg protein)
I	26.01 ± 0.32	476.21 ± 0.76
II	48.01 ± 0.26$^{###}$	220.17 ± 0.49$^{###}$
III	36.2 ± 0.3*	361.24 ± 2.24***
IV	30.91 ± 0.25*	424.88 ± 0.34***
V	28.48 ± 0.14***	470.01 ± 1.27***
VI	28.87 ± 1.13***	454.03 ± 1.48***
VII	24.98 ± 0.45***	485.06 ± 2.14***

Values are expressed as mean ± SEM of 6 rats in each group.
P values: $^{###}$P<0.001 compared with group I
P value: * P<0.05 compared with group II
P value: *** P<0.001 compared with group II



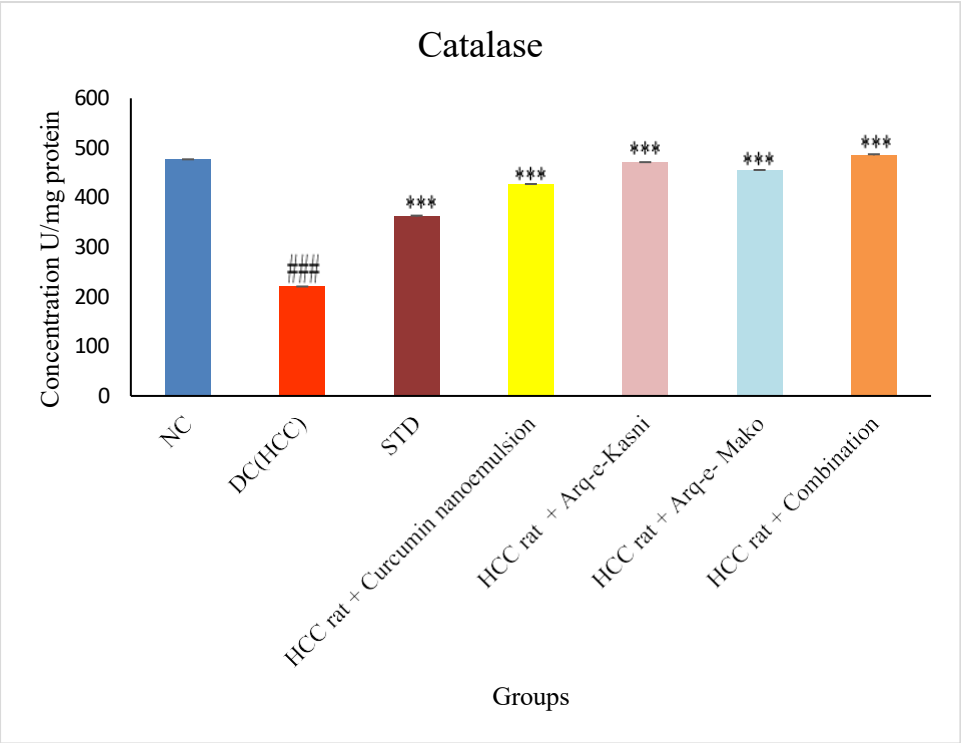
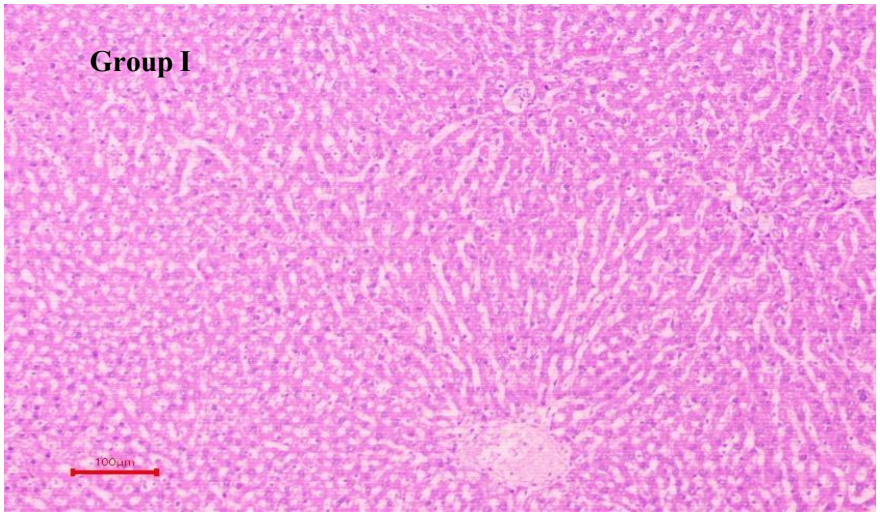
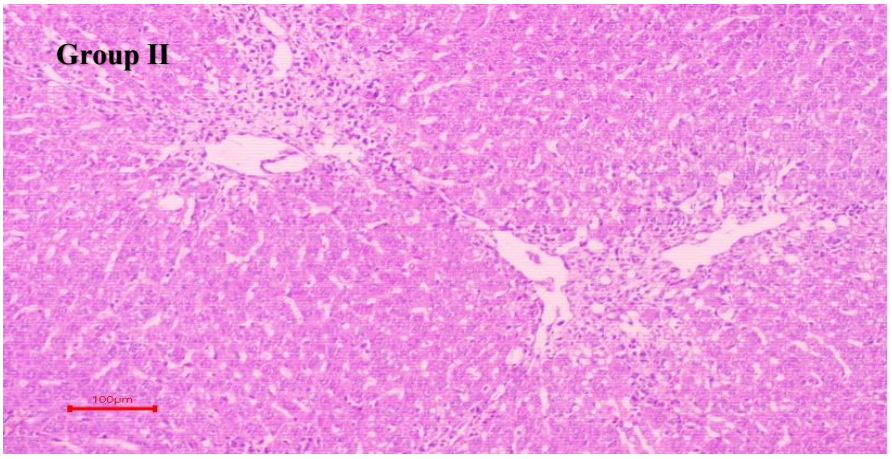


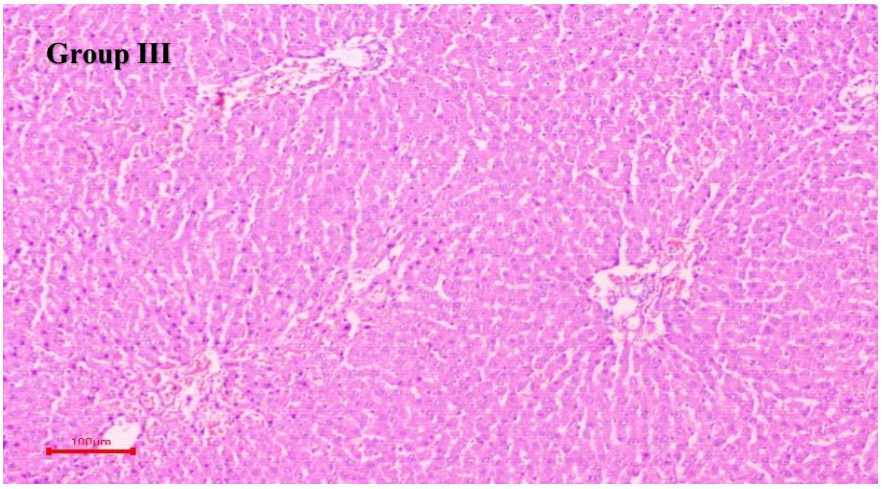
Figure 9: Represent the effect of olive oil-based curcumin nanoemulsion with Ark-e-mako and Ark-e-kasni against diethylnitrosamine induced hepatocellular carcinoma on the level of Lipid peroxidation and catalase in HCC rats.

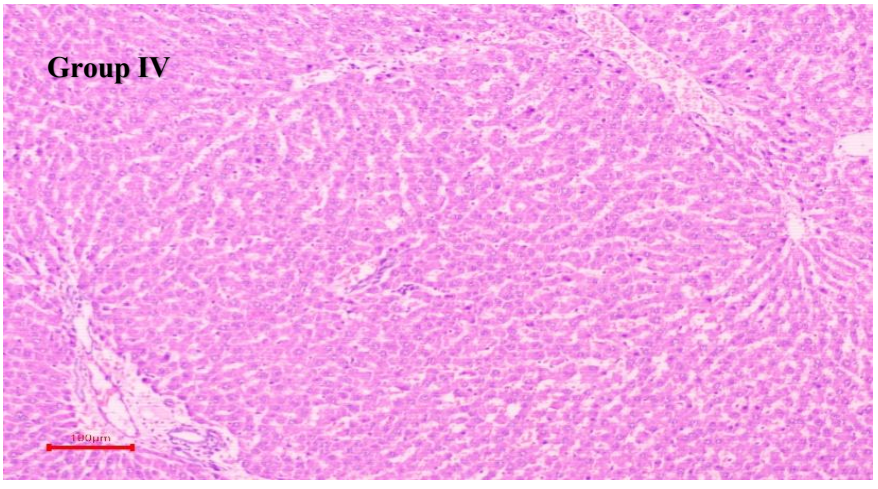
Histopathology:

The results of the tumour marker and blood enzyme testing serve as the foundation for the histopathological analyses **(Figure 10)**. Group I, histology results showed normal hepatic lobule architecture. The hepatocytes appeared normal, presenting as mononucleated cells with regular borders that maintained contact with surrounding cells **(Figure 10 GI)**. Group II histology demonstrates that cells are divided by fibrous septa, cytoplasmic vacuolization of hepatocytes, hepatic necrosis, lymphocyte infiltration and proliferating dysplastic hepatocytes **(Figure 10 GII)**. The Group III rats liver section **(Figure 10 GIII)** displayed sinusoidal dilatation and mild vascular congestion. Additionally, there is a slight periportal lymphocytic infiltrate. The histology of groups IV and V **(Figure 10 GIV)** revealed almost intact architecture with a slight dilation of the central vein and hepatic sinusoids. The periportal triad is surrounded by a lymphocytic infiltration. Hepatic lobules in Group VI histology **(Figure 10 GV)** seemed normal and had reduced infiltration. Hepatic parenchyma appeared normal in Group VII histology **(Figure 10 GVI)**.




Group II
100µm


Group III
100µm


Group IV
100µm

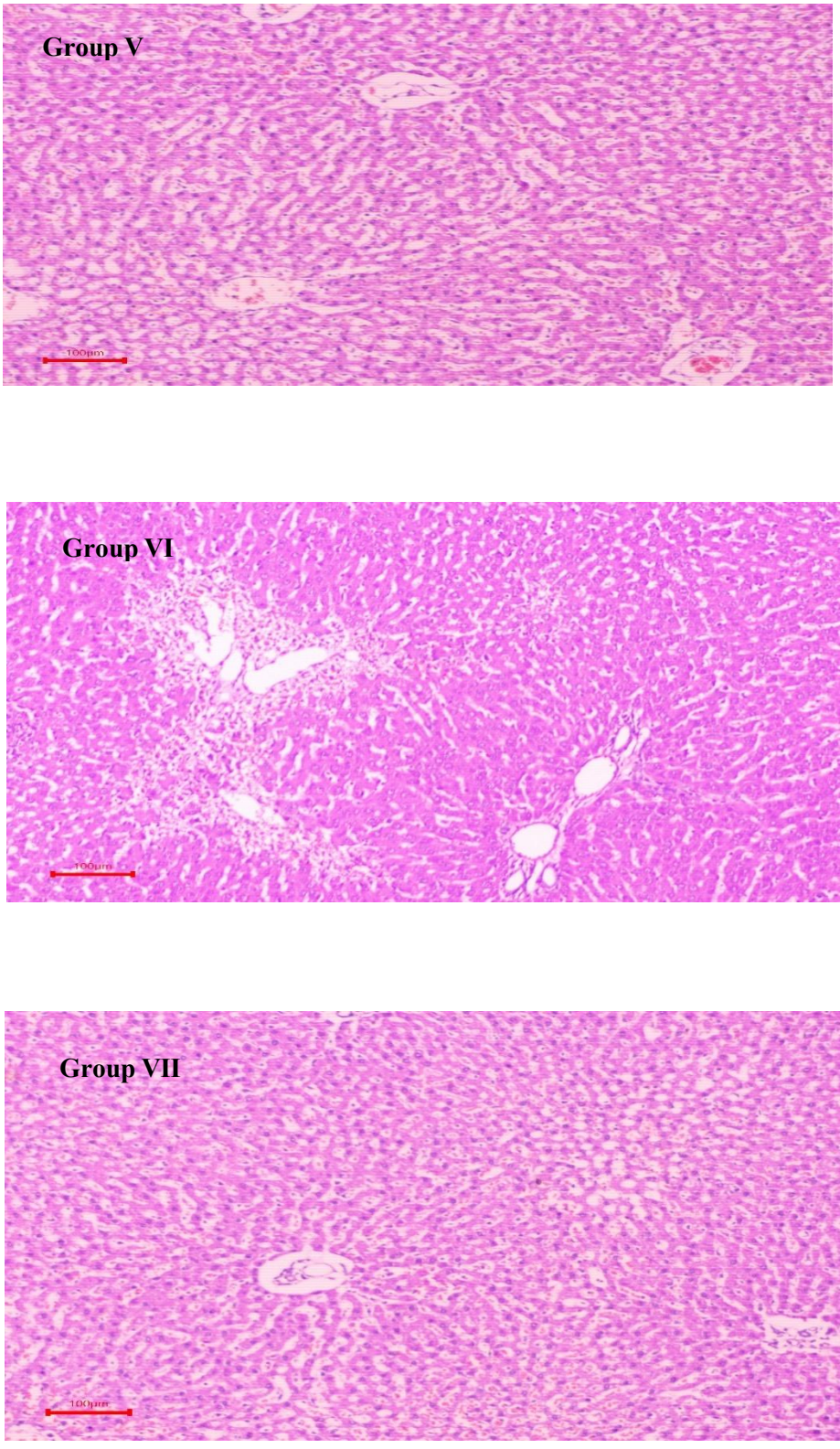


Figure 10: Histopathology of different groups of rat liver tissue

DISCUSSION:

DEN-induced hepatic injury typically results in liver metabolism instability, which causes noticeable alterations in serum enzyme activities [Bulle et. al. 1990]. When liver damage has occurred, aminotransferases (AST and ALT) employed in diagnostic enzymology because they are a trustworthy indicator of liver disease [Whittby et. al. 1984]. Due to their intracellular location in the cytosol, toxicity that affects the liver and causes the cells membrane architecture to break down causes them to leak into serum, where their concentration increases. The elevated activity of these enzymes was considerably reduced in the current study by curcumin nanoemulsion combined with Arq-e-mako and Arq-e-kasni therapy [Shirode et al., 2024]. According to reports, curcumin, Arq-e-mako, and Arq-e-kasni aid in the regeneration of parenchymal cells in the liver, safeguarding membrane integrity

and reducing enzyme leakage [M. Canbek et. al. 2008]. Numerous macromolecular species, including as lipids, proteins, and nucleic acids, are damaged by oxidative stress, leading to significant, interconnected disruptions of cellular metabolism, including lipid peroxidation [selim et al., 2025]. Both human tissues and animals treated with carcinogens developed free radicals and nonradical oxidising species [Sun 1990]. Both endogenous and external sources can produce reactive oxygen species (ROS), which are extremely reactive, poisonous, and mutagenic [Halliwell 1994]. It has been demonstrated that DEN produces free radicals [Halliwell and Gutteridge]. The liver's unrelenting production of free radicals overwhelms the antioxidant status and eventually leads to oxidative stress, which paves the way for the development of cancer. The most researched biologically relevant free radical chain reaction is lipid peroxidation, which is crucial to the development of cancer [Mahendrakumar CB et al., 2004]. According to reports, DEN induction produces lipid peroxidation products such malondialdehyde, which can interact with different molecules to create oxidative stress and carcinogenicity [Hietanen et al., 1987]. LPO levels were found to be elevated during DEN-induced hepatocellular carcinogenesis. The cellular antioxidant defence may be overwhelmed by the unchecked creation of free radicals as a result of this dynamic action [Aeschbach et al., 1994]. Free radicals' involvement in DEN-induced hepatocarcinogenesis has been widely documented. Curcumin, Arq-e-mako and Arq-e-kasni antioxidant properties and free radical scavengers can stop LPO production in its early stages. When compared to animals induced with DEN, animals treated with curcumin nanoemulsion along with Arq-e-mako and Arq-e-kasni showed considerably lower levels of LPO in the liver and serum. This demonstrates the antilipid peroxidative function of curcumin nanoemulsion, Arq-e-kasni, and Arq-e-mako, which is likely mediated by its capacity to scavenge the production of free radicals [Vallianou et al., 2015]. The stimulation of drug-metabolizing enzymes, suppression of prostaglandin synthesis, prevention of carcinogen-induced mutagenesis, and scavenging of free radicals are just a few of the biological functions of antioxidants [Ramsewak et al., 2000]. Antioxidants can shield membranes from ROS toxicity by preventing the production of ROS, stopping ROS attacks, aiding in ROS-induced repair, and supplying cofactors for other antioxidants to operate well [T.P.A Devasagayam et al., 2001]. The availability of these antioxidants is associated with the development of life-threatening illnesses such as hepatocellular carcinoma [Ashrafizadeh et al., 2020]. By preventing the generation of ROS, natural antioxidants can lessen the related intracellular oxidative stress. In the antioxidant system, SOD is the first line of defense against oxidative damage caused by superoxide radicals [Sharifi-Rad et al., 2020]. The conversion of superoxide radicals to hydrogen peroxide and water is catalysed by superoxide dismutase [Bhattacharyya et al., 2014]. Moreover, the conversion of H2O2 into innocuous byproducts is catalysed by CAT or GSH.

The tripeptide glutathione, which contains cysteine, is necessary to keep cells in their normal reduced condition and to mitigate all the negative consequences of oxidative stress. The detoxification of both endogenous and foreign substances is one of the numerous cellular functions that GSH is thought to be engaged in. The huge nucleophilic pool of GSH may interact with the electrophilic carcinogen DEN, decreasing the interaction between the macromolecule and carcinogen [Kenneth A. Conklin 2004]. When compared to DEN-induced animals, the treatment group that received the Curcumin nanoemulsion, Arq-e-Mako, and Arq-e-Kasni had a significantly higher level of GSH in the liver, which is consistent with the theory of attenuating the DNA–carcinogen interaction and preventing a favourable environment for carcinogenesis. Tumour cells showed decreases in the activities of SOD, CAT, GPx, GR, and GSH. It is hypothesised that substances capable of scavenging the body's excess free radicals will prevent the development of cancer [Balaban et al., 2005]. These investigations corroborate our findings because we observed that animals treated with carcinogens had significantly lower levels of antioxidant enzyme activity in their serum and liver compared to normal animals. However, as compared to animals given the carcinogen alone, the livers of animals given both Curcumin nanoemulsion, Arq-e-Mako, Arq-e-Kasni, and the carcinogen showed a considerable rise in the activities of antioxidant enzymes.

The prevalence of apoptotic morphological alterations at the cellular level was further confirmed by ultra-structural investigations. The cytoplasm and nuclei in the control mice were normal. Multiple irregularly shaped nuclei near each other with irregular cytoplasm were observed in the DEN-induced mice, which may have resulted from the increased production of free radicals after DEN administration [Hussein et al., 2026]. The vehicle-treated mice had normal hepatocytes, while the DEN-treated animals had altered hepatocyte architecture. This indicates that the DEN causes intracellular damage to the liver cell, finally demonstrating its hazardous nature at the dosage. The liver cells of rats treated with DEN + methotrexate showed morphological alterations indicative of apoptosis, suggesting that methotrexate may cause apoptosis. HCC Rats treated with Curcumin nanoemulsion, Arq-e-kasni, and Arq-e-mako showed liver cells with condensed chromatin and a shrunken nucleus undergoing apoptosis. Therefore, it is clear from the ultrastructural study’s findings that this combination can induce death in cancer cells.

The current study concludes by showing that the combination therapy has strong antioxidant and free radical scavenging properties. The findings clearly show that therapy with Curcumin nanoemulsion, Arq-e-kasni, and Arq-e-mako can modulate LPO levels and considerably boost endogenous antioxidant defense mechanisms in DEN-induced hepatocellular carcinogenesis. Additionally, our findings demonstrate that combination therapy avoided the notable rise in serum markers alpha feto protein and carcinoembryonic antigen. This suggests that Curcumin nanoemulsion could be developed as an efficient chemotherapeutic drug in combination with Arq-e-kasni and Arq-e-mako.

CONCLUSION:

Curcumin being hydrophobic is poorly absorbed difficult to incorporate in aqueous formulation systems. For this

reason, the curcumin was formulated as olive oil-based nano emulsion form. The present study showed that optimized formulation has mean particle size about 200 nm and zeta potential of −13.76 mV which indicates the development of a nanosized formulation with good physicochemical characteristics.
Moreover, the marked reduction in the levels of the tumour linked markers alpha-fetoprotein (AFP) and carcinoembryonic antigen (CEA) in the treatment groups further validates the beneficial effect of the optimised formulation on the pathological alterations related to the experimental disease state. These biochemical observations were further supported by histological observation which indicated improvement in cellular architecture and repair of tissue structure as compared to disease control group.
The aggregate results demonstrated that the optimized formulation, when used in conjunction with Arq-e-Mako and Arq-e-Kasni, showed improved hepatic functions and anticancer efficacy by improving body weight, liver function biomarkers, tumor-associated indicators, and histological modifications. Consequently, the formulation might serve as a promising method for treating experimentally produced liver disorders, however more investigation is essential to clarify the mechanism of action, long-term safety, pharmacokinetics, and therapeutic efficacy of the formulation.

ACKNOWLEDGEMENTS
We are thankful to the Mahatma Gandhi Institute of Pharmacy and Faculty of Pharmacy Integral University Lucknow for providing suitable facilities and support for the successful completion of this study (IU/R&D/2026-MCN0005046).

CONFLICT OF INTEREST
The authors declare no conflicts of interest relevant to this article.

REFERENCES:
1. Aeschbach, R., Löliger, J., Scott, B. C., Murcia, A., Butler, J., Halliwell, B., & Aruoma, O. I. (1994). Antioxidant actions of thymol, carvacrol, 6-gingerol, zingerone and hydroxytyrosol. Food and chemical toxicology, 32(1), 31-36.
2. Ahmad, N., Ahmad, R., Al-Qudaihi, A., Alaseel, S. E., Fita, I. Z., Khalid, M. S., & Pottoo, F. H. (2019). Preparation of a novel curcumin nanoemulsion by ultrasonication and its comparative effects in wound healing and the treatment of inflammation. RSC advances, 9(35), 20192-20206.
3. Ahmad, U., Akhtar, J., Singh, S. P., Badruddeen, Ahmad, F. J., Siddiqui, S., & Wahajuddin. (2018). Silymarin nanoemulsion against human hepatocellular carcinoma: development and optimization. Artificial cells, nanomedicine, and biotechnology, 46(2), 231-241.
4. Akhtar, J. (2015). Novel oral nanoemulsion based drug delivery system of antidiabetic drugs (Doctoral dissertation, dissertation).
5. Akhtar, J., Hussain Siddiqui, H., Fareed, S., & Aqil, M. (2014). Nanomulsion as a carrier for efficient delivery of metformin. Current drug delivery, 11(2), 243-252.
6. Ashrafizadeh, M., Rafiei, H., Mohammadinejad, R., Afshar, E. G., Farkhondeh, T., & Samarghandian, S. (2020). Potential therapeutic effects of curcumin mediated by JAK/STAT signaling pathway: a review. Phytotherapy Research, 34(8), 1745-1760.
7. Balaban, R. S., Nemoto, S., & Finkel, T. (2005). Mitochondria, oxidants, and aging. cell, 120(4), 483-495.
8. Balogh, J., Victor III, D., Asham, E. H., Burroughs, S. G., Boktour, M., Saharia, A., ... & Monsour Jr, H. P. (2016). Hepatocellular carcinoma: a review. Journal of hepatocellular carcinoma, 41-53.
9. Barenholz, Y. C. (2012). Doxil®—The first FDA-approved nano-drug: Lessons learned. Journal of controlled release, 160(2), 117-134.
10. Bharti, A. C. (2003). Anticancer potential of curcumin: preclinical and clinical studies. Anticancer research.
11. Bhattacharyya, A., Chattopadhyay, R., Mitra, S., & Crowe, S. E. (2014). Oxidative stress: an essential factor in the pathogenesis of gastrointestinal mucosal diseases. Physiological reviews, 94(2), 329-354.
12. Bulle, F., Mavier, P., Zafrani, E. S., Preaux, A. M., Lescs, M. C., Siegrist, S., ... & Guellaën, G. (1990). Mechanism of γ-glutamyl transpeptidase release in serum during intrahepatic and extrahepatic cholestasis in the rat: A histochemical, biochemical and molecular approach. Hepatology, 11(4), 545-550.
13. Canbek, M., Uyanoglu, M., Bayramoglu, G., Senturk, H., Erkasap, N., Koken, T., ... & Baser, K. H. C. (2008). Effects of carvacrol on defects of ischemia-reperfusion in the rat liver. Phytomedicine, 15(6-7), 447-452.
14. Conklin, K. A. (2004). Chemotherapy-associated oxidative stress: impact on chemotherapeutic effectiveness. Integrative cancer therapies, 3(4), 294-300.
15. Devasagayam, T. P., Kamat, J. P., & Sreejayan, N. (2001). Antioxidant action of curcumin. Micronutrients and health: molecular biological mechanisms, 42-59.
16. Goc, Z., Szaroma, W., Kapusta, E., & Dziubek, K. (2017). Protective effects of melatonin on the activity of SOD, CAT, GSH-Px and GSH content in organs of mice after administration of SNP. Chin J Physiol, 60(1), 1-10.
17. Hietanen, E., Ahotupa, M., Bartsch, H., Bereziat, J. C., Bussacchini, V., Camus, A. M., & Wild, H. (1987). Lipid peroxidation and chemically induced cancer in rats fed lipid rich diet. Carcinogenesis and tumor progression, 4, 9-16.
18. Hussein, J., El-Daly, S. M., Medhat, D., El-Bana, M. A., Morsy, S. M., Omara, E., & Elimam, H. (2026). EPA-loaded silica nanoemulsions attenuate DEN-induced hepatic fibroinflammation by modulating homocysteine, PKCα/NF-κB, and Nrf2 signaling. Naunyn-Schmiedeberg's Archives of Pharmacology, 1-15.

19. King J (1965) The transferase-alanine and aspartate transaminase. In: King J (ed) Practical clinical enzymology. D Van Nostrand Company Ltd, London, pp 121–138
20. Kommuru, T., Gurley, B., Khan, M. A., & Reddy, I. K. (2001). Self-emulsifying drug delivery systems (SEDDS) of coenzyme Q10: formulation development and bioavailability assessment. International journal of pharmaceutics, 212(2), 233-246.
21. Lawrence, M. J., & Rees, G. D. (2000). Microemulsion-based media as novel drug delivery systems. Advanced drug delivery reviews, 45(1), 89-121.
22. Mahendrakumar, C. B., Vrushabendra Swamy, B. M., Archana, D. V., & Somasekhar Rao, K. S. (2004). Hepatoprotective activity of Arq-e-Mahu and Arq-e-Khasni (Unani formulation) against paracetamol induced hepatotoxicity in albino rats. Indian Journal of Traditional Knowledge, 3(4), 430–434.
23. Parveen, S., & Sahoo, S. K. (2011). Long circulating chitosan/PEG blended PLGA nanoparticle for tumor drug delivery. European journal of pharmacology, 670(2-3), 372-383.
24. Parween, A., & Begum, W. (2017). Effect of ARQ MAKO and sharbat kasni in Waram Al rahim (pelvic inflammatory disease): an observational clinical trial. International Journal for Advance Research and Development, 2(9), 7-13.
25. Rageh, M. M., Abdelmoneam, E. A., Sharaky, M., & Mohamad, E. A. (2023). Physico-chemical properties of curcumin nanoparticles and its efficacy against Ehrlich ascites carcinoma. Scientific Reports, 13(1), 20637.

26. Ramsewak, R. S., DeWitt, D. L., & Nair, M. G. (2000). Cytotoxicity, antioxidant and anti-inflammatory activities of curcumins I–III from Curcuma longa. Phytomedicine, 7(4), 303-308.
27. Selim, N. M., El-Hawary, S. S., El Zalabani, S. M., Shamma, R. N., Mahdy, N. E. S., Sherif, N. H., ... & Fahmy, H. A. (2025). Washingtonia robusta H. Wendl Leaf Metabolites Potentiate the Radiosensitivity of Hepatocellular Carcinoma Through Ki67 and PARP Inhibition. Integrative Cancer Therapies, 24, 15347354241308858.
28. Sharifi-Rad, J., Rayess, Y. E., Rizk, A. A., Sadaka, C., Zgheib, R., Zam, W., ... & Martins, N. (2020). Turmeric and its major compound curcumin on health: bioactive effects and safety profiles for food, pharmaceutical, biotechnological and medicinal applications. Frontiers in pharmacology, 11, 01021.
29. Shirode, D. S., Raut, D. J., & Sarasawat, N. (2024). Effect of Niosomal Encapsulation of Quercetin and Silymarin and their Combination on Dimethylnitrosoamine-induced and Phenobarb italpromoted Hepatocellular Carcinoma in Rat Model. Current Drug Discovery Technologies, 21(5), 43-55.
30. Srimal, R. C., & Dhawan, B. N. (1973). Pharmacology of diferuloyl methane (curcumin), a non-steroidal anti-inflammatory agent. Journal of pharmacy and pharmacology, 25(6), 447-452.
31. Talerman, A., Van Der Pompe, W. B., Haije, W. G., Baggerman, L., & Boekestein-Tjahjadi, H. M. (1977). Alpha-foetoprotein and carcinoembryonic antigen in germ cell neoplasms. British journal of cancer, 35(3), 288-291.
32. Vallianou, N. G., Evangelopoulos, A., Schizas, N., & Kazazis, C. (2015). Potential anticancer properties and mechanisms of action of curcumin. Anticancer research, 35(2), 645-651.
33. Whittby LG, Perey-Robb IW, Smith AT (1984) Enzymes tests in diagnosis, Lecture notes in clinical chemistry, 3rd edn. Black Well Scientific Publications, London, pp 138–169
34. Zaafar, Dalia, et al. "Preparation and characterization of Sorafenib nano-emulsion: impact on pharmacokinetics and toxicity; an in vitro and in vivo study." Drug Delivery and Translational Research 14.11 (2024): 3089-3111.
35. Zeenat, F. (2019). Resolution of Hemorrhagic Ovarian Cyst by Unani Formulations. Int. J. of AYUSH Case Reports April–June, 3(2).